Indirect Measurement of Switch Terms of a Vector Network Analyzer With Reciprocal Devices

Ziad Hatab, *Student Member, IEEE*, Michael Ernst Gadringer, *Senior Member, IEEE*, and Wolfgang Bösch, *Fellow, IEEE*

***Abstract*— This letter presents an indirect method for measuring the switch terms of a vector network analyzer (VNA) using at least three reciprocal devices, which do not need to be characterized beforehand. This method is particularly suitable for VNAs that use a three-sampler architecture, which allows for applying first-tier calibration methods based on the error box model. The proposed method was experimentally verified by comparing directly and indirectly measured switch terms and performing a multiline thru–reflect–line (TRL) calibration.**

***Index Terms*— Calibration, microwave measurement, vector network analyzer (VNA).**

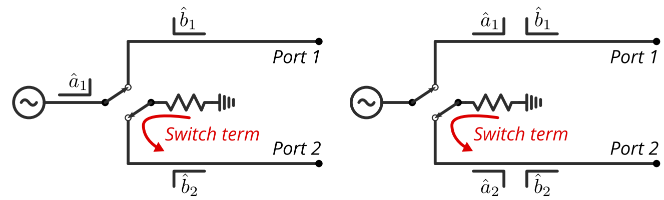

(a) (b)

Fig. 1. Illustration of three- (a) and four-sampler (b) architectures of a VNA. Both the diagrams depict source driving in the forward direction.

I. Introduction

CALIBRATION of vector network analyzers (VNAs) is essential to eliminate systematic errors and define the reference plane to the device under test (DUT). The short–open–load–thru (SOLT) method is the most common calibration method based on the 12-term error model of a two-port VNA. However, it needs fully characterized standards. In [1], the short–open–load–reciprocal (SOLR) method was introduced based on the error box model, where a transmissive reciprocal device replaces the thru standard. Other advanced self-calibration methods, including thru–reflect–line (TRL), multiline TRL, line-reflect-match (LRM), and line-reflect-reflect-match (LRRM) [2], [3], [4], [5], are also based on the error box model.

Calibration methods based on the error box model require a four-sampler VNA, while the 12-term error model can still be used in the three-sampler VNA. Fig. 1 shows the two architectures for a two-port VNA. In the three-sampler VNA, we do not sample the reflected wave of the termination load of the nondriving port. This reflection coefficient is called the switch term [6]. There are two switch terms for the two-port configuration and N switch terms for the general multiport configuration, where N is the number of ports.

Given that the termination of the nondriving ports remains constant during measurement, the switch terms introduce systematic error and only need to be measured once. These terms can be considered as part of the calibration coefficients through the conversion relationships between the 12-term and error box models [6], [7], [8], [9].

For three-sampler VNAs, self-calibration based on the error box model is not possible as switch terms cannot be directly measured. Instead, an SOLT calibration or equivalent can be performed using known standards with the 12- or 10-term model (ignoring crosstalk), as explained in [10] for multiport VNAs. In addition, error box calibration can be performed as a second-tier after SOLT calibration [11]. However, SOLT calibration requires characterized standards, which contradicts the purpose of self-calibration using partially defined standards.

This letter aims to introduce a new method to indirectly measure the switch terms using at least three transmissive reciprocal devices, which do not need to be characterized beforehand. The proposed method enables the usage of error box calibration methods in three-sampler VNAs without requiring any prior calibration.

Manuscript received 12 June 2023; revised 28 July 2023; accepted 24 August 2023. Date of publication 29 September 2023; date of current version 8 November 2023. This work was supported by the Christian Doppler Research Association and the Austrian Federal Ministry for Digital and Economic Affairs and the National Foundation for Research, Technology, and Development. *(Corresponding author: Ziad Hatab.)*

The authors are with the Institute of Microwave and Photonic Engineering, Christian Doppler Laboratory for Technology-Guided Electronic Component Design and Characterization (TONI), Graz University of Technology, 8010 Graz, Austria (e-mail: z.hatab@tugraz.at; michael.gadringer@tugraz.at; wbosch@tugraz.at).

Data is available online at https://github.com/ZiadHatab/vna-switch-terms

Color versions of one or more figures in this letter are available at https://doi.org/10.1109/LMWT.2023.3311032.

Digital Object Identifier 10.1109/LMWT.2023.3311032

II. Mathematical Formulation

A. Problem Statement

In a two-port VNA, when all the four waves are sampled in both forward and reverse directions, the measured S-parameters are described using the following notation [12]:

$$\begin{bmatrix}\hat{b}_{11} & \hat{b}_{12}\\ \hat{b}_{21} & \hat{b}_{22}\end{bmatrix} = \boldsymbol{S}\begin{bmatrix}\hat{a}_{11} & \hat{a}_{12}\\ \hat{a}_{21} & \hat{a}_{22}\end{bmatrix} \tag{1}$$

where $\hat{a}_{ij}$ and $\hat{b}_{ij}$ represent the sampled incident and reflected waves, respectively, at port-i when driven by port-j.

In a three-sampler VNA, the waves $\hat{a}_{12}$ and $\hat{a}_{21}$ are not measured due to a lack of dedicated receivers. The measured incident waves in (1) can be split into two matrices as follows:

$$\begin{bmatrix}\hat{b}_{11} & \hat{b}_{12}\\ \hat{b}_{21} & \hat{b}_{22}\end{bmatrix} = \boldsymbol{S}\begin{bmatrix}1 & \frac{\hat{a}_{12}}{\hat{a}_{22}}\\ \frac{\hat{a}_{21}}{\hat{a}_{11}} & 1.\end{bmatrix}\begin{bmatrix}\hat{a}_{11} & 0\\ 0 & \hat{a}_{22}\end{bmatrix}. \tag{2}$$

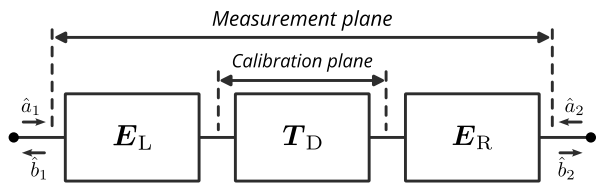

Fig. 2. Two-port VNA error box model.

By taking the inverse of the diagonal matrix on the right-hand side of (2), we obtain the conventionally measured ratios

$$\begin{bmatrix} \frac{\hat{b}_{11}}{\hat{a}_{11}} & \frac{\hat{b}_{12}}{\hat{a}_{22}} \\ \frac{\hat{b}_{21}}{\hat{a}_{11}} & \frac{\hat{b}_{22}}{\hat{a}_{22}} \end{bmatrix} = \boldsymbol{S}\begin{bmatrix} 1 & \frac{\hat{a}_{12}}{\hat{a}_{22}} \\ \frac{\hat{a}_{21}}{\hat{a}_{11}} & 1 \end{bmatrix}. \tag{3}$$

If we define the ratios on the left-hand side of (3) as the measured S-parameters, we can then rewrite the remaining ratios on the right-hand side as follows:

$$\begin{bmatrix} \overline{S}_{11} & \overline{S}_{12} \\ \overline{S}_{21} & \overline{S}_{22} \end{bmatrix} = \boldsymbol{S}\begin{bmatrix} 1 & \overline{S}_{12}\Gamma_{12} \\ \overline{S}_{21}\Gamma_{21} & 1 \end{bmatrix} \tag{4}$$

where $\overline{S}_{ij}$ represents the measured S-parameters, and Γ_{ij} represents the switch terms of the VNA

$$\overline{S}_{ij} = \frac{\hat{b}_{ij}}{\hat{a}_{jj}}, \qquad \Gamma_{ij} = \frac{\hat{a}_{ij}}{\hat{b}_{ij}}. \tag{5}$$

The switch terms are formed by the ratios of the receivers of the nondriving port. Therefore, they are independent of the measured DUT, as any influence introduced by the DUT will be seen equally by both the receivers. In the special case where the measured two-port device is transmissionless, the switch terms Γ_{ij} do not influence the measurements as $\overline{S}_{21} = \overline{S}_{12} = 0$.

Using a four-sampler VNA, we can directly measure Γ_{ij} by connecting any transmissive device and calculating the ratios as defined in (5). However, a three-sampler VNA can only measure $\overline{S}_{ij}$.

B. Proposed Indirect Measurement of the Switch Terms

Fig. 2 shows the error box model of a two-port VNA. Using T-parameters, the measured DUT is given in terms of wave quantities as follows [12]:

$$\begin{bmatrix} \hat{a}_{11} & \hat{a}_{12} \\ \hat{b}_{11} & \hat{b}_{12} \end{bmatrix} = \boldsymbol{E}_\mathrm{L}\boldsymbol{T}_\mathrm{D}\boldsymbol{E}_\mathrm{R}\begin{bmatrix} \hat{a}_{21} & \hat{a}_{22} \\ \hat{b}_{21} & \hat{b}_{22} \end{bmatrix} \tag{6}$$

where $\boldsymbol{E}_\mathrm{L}$ and $\boldsymbol{E}_\mathrm{R}$ are the left and right error boxes, respectively, and $\boldsymbol{T}_\mathrm{D}$ is the actual DUT.

We split the wave matrices in (6) into two matrices as follows:

$$\begin{bmatrix} 1 & \frac{\hat{a}_{12}}{\hat{b}_{12}} \\ \frac{\hat{b}_{11}}{\hat{a}_{11}} & 1 \end{bmatrix}\begin{bmatrix} \hat{a}_{11} & 0 \\ 0 & \hat{b}_{12} \end{bmatrix} = \boldsymbol{E}_\mathrm{L}\boldsymbol{T}_\mathrm{D}\boldsymbol{E}_\mathrm{R}\begin{bmatrix} \frac{\hat{a}_{21}}{\hat{b}_{21}} & 1 \\ 1 & \frac{\hat{b}_{22}}{\hat{a}_{22}} \end{bmatrix}\begin{bmatrix} \hat{b}_{21} & 0 \\ 0 & \hat{a}_{22} \end{bmatrix}. \tag{7}$$

The above expression can be simplified by multiplying the inverse of the diagonal matrix at the right-hand side. This step reduces all the wave quantities into ratios as follows:

$$\begin{bmatrix} 1 & \frac{\hat{a}_{12}}{\hat{b}_{12}} \\ \frac{\hat{b}_{11}}{\hat{a}_{11}} & 1 \end{bmatrix}\begin{bmatrix} \frac{\hat{a}_{11}}{\hat{b}_{21}} & 0 \\ 0 & \frac{\hat{b}_{12}}{\hat{a}_{22}} \end{bmatrix} = \boldsymbol{E}_\mathrm{L}\boldsymbol{T}_\mathrm{D}\boldsymbol{E}_\mathrm{R}\begin{bmatrix} \frac{\hat{a}_{21}}{\hat{b}_{21}} & 1 \\ 1 & \frac{\hat{b}_{22}}{\hat{a}_{22}} \end{bmatrix}. \tag{8}$$

The final simplification is to replace the ratios with the definitions established in (5). The rearranged expression is presented in the following equation:

$$\begin{bmatrix} 1 & \Gamma_{12} \\ \overline{S}_{11} & 1 \end{bmatrix}\begin{bmatrix} 1/\overline{S}_{21} & 0 \\ 0 & \overline{S}_{12} \end{bmatrix} = \boldsymbol{E}_\mathrm{L}\boldsymbol{T}_\mathrm{D}\boldsymbol{E}_\mathrm{R}\begin{bmatrix} \Gamma_{21} & 1 \\ 1 & \overline{S}_{22} \end{bmatrix}. \tag{9}$$

Our goal is to extract Γ_{21} and Γ_{12} without prior knowledge of the error boxes or the DUT. We assume the DUT is a reciprocal device, i.e., $\det(\boldsymbol{T}_\mathrm{D}) = 1$. By applying the determinate operator to (9) and using the property that $\det(\boldsymbol{AB}) = \det(\boldsymbol{A})\det(\boldsymbol{B})$, we arrive at the following:

$$(1 - \overline{S}_{11}\Gamma_{12})\frac{\overline{S}_{12}}{\overline{S}_{21}} = \underbrace{\det(\boldsymbol{E}_\mathrm{L})\det(\boldsymbol{E}_\mathrm{R})}_{=c\text{ (constant)}}(\Gamma_{21}\overline{S}_{22} - 1). \tag{10}$$

The above expression can be simplified as follows:

$$\frac{\overline{S}_{12}}{\overline{S}_{21}} - \overline{S}_{11}\frac{\overline{S}_{12}}{\overline{S}_{21}}\Gamma_{12} - \overline{S}_{22}c\Gamma_{21} + c = 0. \tag{11}$$

From (11), we can recognize that we have a linear equation in three unknowns: Γ_{12}, $c\Gamma_{21}$, and c. Therefore, if we measure at least three unique transmissive reciprocal devices, we arrive at the following linear system of equations:

$$\underbrace{\begin{bmatrix} -\overline{S}_{11}^{(1)}\frac{\overline{S}_{12}^{(1)}}{\overline{S}_{21}^{(1)}} & -\overline{S}_{22}^{(1)} & 1 & \frac{\overline{S}_{12}^{(1)}}{\overline{S}_{21}^{(1)}} \\ \vdots & \vdots & \vdots & \vdots \\ -\overline{S}_{11}^{(M)}\frac{\overline{S}_{12}^{(M)}}{\overline{S}_{21}^{(M)}} & -\overline{S}_{22}^{(M)} & 1 & \frac{\overline{S}_{12}^{(M)}}{\overline{S}_{21}^{(M)}} \end{bmatrix}}_{\boldsymbol{H}}\begin{bmatrix} \Gamma_{12} \\ c\Gamma_{21} \\ c \\ 1 \end{bmatrix} = \boldsymbol{0} \tag{12}$$

where $M \geq 3$ is the number of measured reciprocal devices.

To solve for the unknowns in (12), we need to find the nullspace of $\boldsymbol{H}$. The sensitivity of the solution depends on the uniqueness of the measured reciprocal devices, which can be quantified by the condition number of $\boldsymbol{H}$ [13], as follows:

$$\kappa(\boldsymbol{H}) = \|\boldsymbol{H}\|_F\left\|\boldsymbol{H}^+\right\|_F = \frac{\sigma_1}{\sigma_r} \tag{13}$$

where $(\cdot)^+$ is the pseudoinverse, and $\|\cdot\|_F$ is the Frobenius norm. The values σ_1 and σ_r correspond to the largest and smallest nonzero singular values (in decreasing order), respectively, which are obtained from the singular value decomposition (SVD) [14]. In order for $\boldsymbol{H}$ to be solvable, it has to have a rank of 3, hence $\sigma_r = \sigma_3$. The condition number is a relative metric, where the nullspace solution becomes more sensitive as the condition number increases.

The nullspace solution is represented by the right singular vector that corresponds to the zero singular value. Since $\boldsymbol{H}$ has a rank of 3, the nullspace corresponds to the fourth right singular vector, $\boldsymbol{v}_4$. However, singular vectors are only unique up to a scalar multiple, as given below

$$\boldsymbol{v}_4 = \begin{bmatrix} v_{41} \\ v_{42} \\ v_{43} \\ v_{44}. \end{bmatrix} = \alpha\begin{bmatrix} \Gamma_{12} \\ c\Gamma_{21} \\ c \\ 1. \end{bmatrix} \quad \forall\alpha \neq 0. \tag{14}$$

Therefore, the switch terms are solved as follows:

$$\Gamma_{12} = \frac{v_{41}}{v_{44}}, \qquad \Gamma_{21} = \frac{v_{42}}{v_{43}}. \tag{15}$$

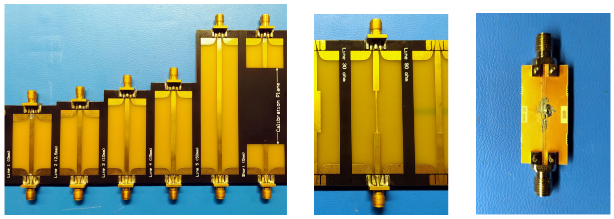

(a) (b) (c)

Fig. 3. Measured structures. (a) Microstrip line multiline TRL kit (50 Ω). (b) Stepped impedance line (90 Ω). (c) Series-shunt 100 Ω circuit.

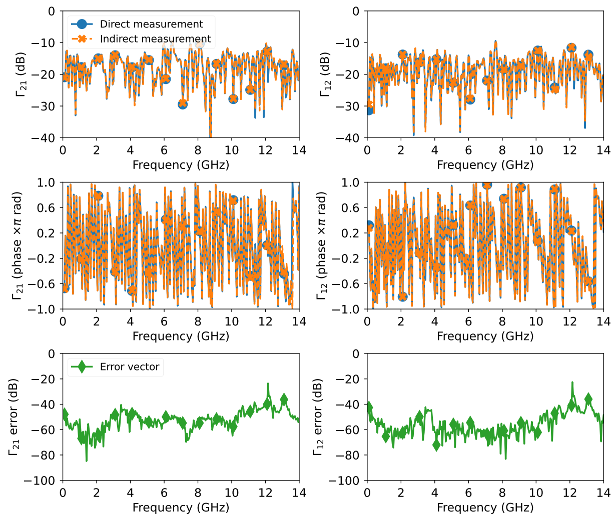

Fig. 4. Comparison of direct and indirect measurements of the switch terms.

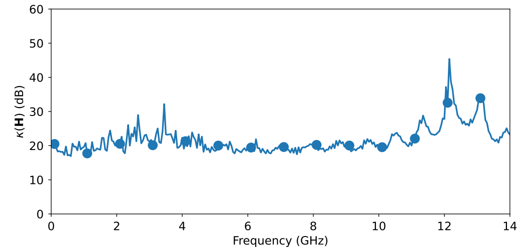

Fig. 5. Condition number of the system matrix in (12).

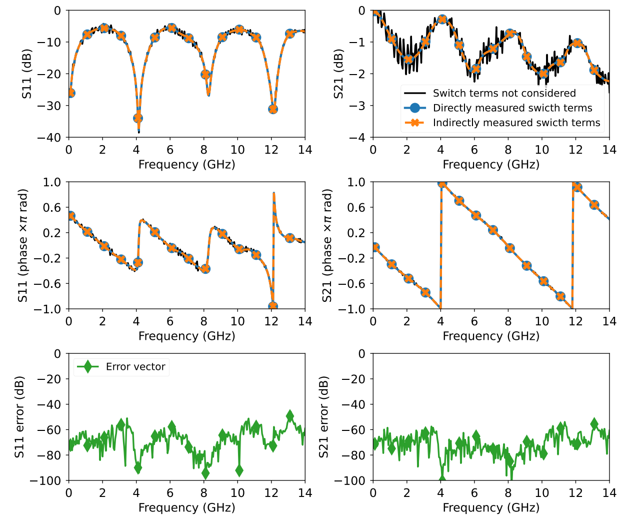

Fig. 6. Results of the multiline TRL calibrated stepped impedance line.

III. Experiment

The experiment had two parts. First, we tested our method for extracting switch terms using only three of the four available receivers in a VNA. We compared the results to switch terms computed directly using the fourth receiver. Second, we performed a multiline TRL calibration using both directly and indirectly computed switch terms. We compared the results by calibrating a stepped impedance line.

The R&S ZVA, a four-sampler VNA, was used in the experiment. The reciprocal devices consisted of a line standard from the multiline TRL kit (50 mm line) and 100 Ω resistors in a series-shunt (L-circuit) configuration. We measured the L-circuit twice by flipping the ports since it is asymmetric. The L-circuit was chosen because it offers unique rows in the system matrix in (12) and can cover lower frequency due to the usage of resistors.

We used microstrip lines on an FR4 substrate with a trace width of 3 mm and a substrate height of 1.55 mm for the multiline TRL kit. The relative lengths of the lines were {0, 2.5, 10, 15, 50} mm, with the reflect standard implemented as a short. All the standards are shown in Fig. 3.

To extract the switch terms, we measured the reciprocal devices and processed the data using the *scikit-rf* package in Python [15]. The results obtained by direct wave ratio computation with the fourth receiver were compared with the indirect method, and the error between the two methods is shown in Fig. 4. The error metric is defined as follows:

$$\text{Error}_{ij}\ (\text{dB}) = 20\log_{10}\left|\Gamma_{ij}^{(\text{direct})} - \Gamma_{ij}^{(\text{indirect})}\right|. \tag{16}$$

The results demonstrate low error and a minor spike around 12 GHz, which can be explained by analyzing the condition number of the system matrix shown in Fig. 5. The condition number demonstrates an increase in sensitivity around 12 GHz, indicating that at these frequencies, the used standards exhibit a similar frequency response.

Finally, we performed multiline TRL calibration based on the algorithm in [16] and [17]. Fig. 6 shows the calibrated results of a stepped impedance line in different scenarios: ignoring the switch terms, directly measuring the switch terms, and indirectly measuring the switch terms, as well as the error between the methods. The results in Fig. 6 show that ignoring the switch terms results in noise-like behavior on the traces, but both directly and indirectly measured switch terms give comparable results.

IV. Conclusion

This letter presented a new technique for measuring switch terms of a three-sampler VNA, which entails measuring three transmissive reciprocal devices. We compared the new indirect method to the direct approach using the fourth receiver on a four-sampler VNA. The results obtained using the indirect method were comparable to the direct method. In addition, we demonstrated a first-tier multiline TRL calibration using just three receivers. This method does not require prior knowledge of the reciprocal devices, making it particularly useful for error box calibration methods in multiport VNAs, allowing $N+1$ samplers to replace a dual reflectometer architecture with $2N$ samplers, where N is the number of ports.

REFERENCES

[1] A. Ferrero and U. Pisani, “Two-port network analyzer calibration using an unknown ‘thru,”’ *IEEE Microw. Guided Wave Lett.*, vol. 2, no. 12, pp. 505–507, Dec. 1992, doi: 10.1109/75.173410.

[2] G. F. Engen and C. A. Hoer, “Thru-reflect-line: An improved technique for calibrating the dual six-port automatic network analyzer,” *IEEE Trans. Microw. Theory Techn.*, vol. MTT-27, no. 12, pp. 987–993, Dec. 1979, doi: 10.1109/TMTT.1979.1129778.

[3] R. B. Marks, “A multiline method of network analyzer calibration,” *IEEE Trans. Microw. Theory Techn.*, vol. 39, no. 7, pp. 1205–1215, Jul. 1991, doi: 10.1109/22.85388.

[4] H.-J. Eul and B. Schiek, “Thru-match-reflect: One result of a rigorous theory for de-embedding and network analyzer calibration,” in *1988 18th Eur. Microw. Conf.*, Sep. 1988, pp. 909–914, doi: 10.1109/EUMA.1988.333924.

[5] L. Hayden, “An enhanced line-reflect-reflect-match calibration,” in *Proc. 67th ARFTG Conf.*, Jun. 2006, pp. 143–149, doi: 10.1109/ARFTG.2006.4734364.

[6] R. B. Marks, “Formulations of the basic vector network analyzer error model including switch-terms,” in *Proc. 50th ARFTG Conf. Dig.*, Dec. 1997, pp. 115–126, doi: 10.1109/ARFTG.1997.327265.

[7] S. Vandenberghe, D. Schreurs, G. Carchon, B. Nauwelaers, and W. De Raedt, “Identifying error-box parameters from the twelve-term vector network analyzer error model,” in *Proc. 60th ARFTG Conf. Dig., Fall.*, Dec. 2002, pp. 157–165, doi: 10.1109/ARFTGF.2002.1218697.

[8] L. Hayden, “VNA error model conversion for N-port calibration comparison,” in *Proc. 69th ARFTG Conf.*, Jun. 2007, pp. 1–10, doi: 10.1109/ARFTG.2007.5456343.

[9] J. A. Jargon, D. F. Williams, and A. Sanders, “The relationship between switch-term-corrected scattering-parameters and wave-parameters measured with a two-port vector network analyzer,” *IEEE Microw. Wireless Compon. Lett.*, vol. 28, no. 10, pp. 951–953, Oct. 2018, doi: 10.1109/LMWC.2018.2867076.

[10] A. Ferrero, V. Teppati, M. Garelli, and A. Neri, “A novel calibration algorithm for a special class of multiport vector network analyzers,” *IEEE Trans. Microw. Theory Techn.*, vol. 56, no. 3, pp. 693–699, Mar. 2008, doi: 10.1109/TMTT.2008.916952.

[11] J. A. Jargon and R. B. Marks, “Two-tier multiline TRL for calibration of low-cost network analyzers,” in *46th ARFTG Conf. Dig.*, vol. 28, Nov. 1995, pp. 1–8, doi: 10.1109/ARFTG.1995.327126.

[12] A. Rumiantsev and N. Ridler, “VNA calibration,” *IEEE Microw. Mag.*, vol. 9, no. 3, pp. 86–99, Jun. 2008, doi: 10.1109/MMM.2008.919925.

[13] D. J. Higham, “Condition numbers and their condition numbers,” *Linear Algebra Appl.*, vol. 214, pp. 193–213, Jan. 1995, doi: 10.1016/0024-3795(93)00066-9.

[14] G. Strang, “The fundamental theorem of linear algebra,” *Amer. Math. Monthly*, vol. 100, no. 9, pp. 848–855, Nov. 1993, doi: 10.1080/00029890.1993.11990500.

[15] A. Arsenovic et al., “scikit-RF: An open source Python package for microwave network creation, analysis, and calibration [speaker’s corner],” *IEEE Microw. Mag.*, vol. 23, no. 1, pp. 98–105, Jan. 2022, doi: 10.1109/MMM.2021.3117139.

[16] Z. Hatab, M. Gadringer, and W. Bösch, “Improving the reliability of the multiline TRL calibration algorithm,” in *Proc. 98th ARFTG Microw. Meas. Conf. (ARFTG)*, Jan. 2022, pp. 1–5, doi: 10.1109/ARFTG52954.2022.9844064.

[17] Z. Hatab, M. E. Gadringer, and W. Bösch, “Propagation of linear uncertainties through multiline thru-reflect-line calibration,” *IEEE Trans. Instrum. Meas.*, vol. 72, pp. 1–9, 2023, doi: 10.1109/TIM.2023.3296123.